
0.1 Case studies

Although the theoretical foundation derived above guarantees convergence of the lever arms for the various designs under the stated assumptions, it does not evaluate performance and robustness. To shed light on this, case studies are performed for the GNSS and the MRU lever arm estimation. Data from sea trials with R/V Gunnerus is used for the case studies.

For the GNSS lever arms two different case studies are performed for both the Luenberger observer, and the adaptive design. In the first case study the GPS data are simulated, using sea trial data. That is, the linear velocity, and Euler angles (?) from the sea trial are used, and the GPS data is simulated based on that data (see Section 0.1.1). The reason GPS data is simulated is done to avoid signal synchronization and consistency issues in the input data. For the second case study the actual GPS data is used.

For the MRU lever arm estimation one case study is performed. That is with the Luenberger observer of Section ?? on real data.

0.1.1 Case studies - GNSS (GPS) lever arms

Gunnerus data In the August sea trials three turning maneuvers were performed. Two of them has a constant yaw rate, but with different rates, and the last one has a varying yaw rate. The intention was to use these maneuvers for lever arm verification. Unfortunately, the GPS measurements from MARINTEK are poor during those maneuvers (low resolution), and only the DP system GPS measurements are available. Since only one GPS measurement series is available for these maneuvers, a turning circle performed by MARINTEK is used instead. This still only gives one GPS measurement series, but all the other signals used (angular rates and linear velocities) are collected from MARINTEK measurements, so this reduce the problem of synchronization issues, since all the data is collected from the same source.

For the GPS case studies, data from a so called "turning circle" maneuver is applied. The vessel turns with a constant rudder angle of 20 degrees on the rudders. The maneuver was performed by MARINTEK in the November sea trials. The GPS measurements available are the MARINTEK measurements, and the values for roll, pitch, and yaw rate from this maneuver are shown in Figure 1 below. The roll and pitch rates oscillate about a zero mean, whereas the yaw rate oscillates around a nonzero mean.

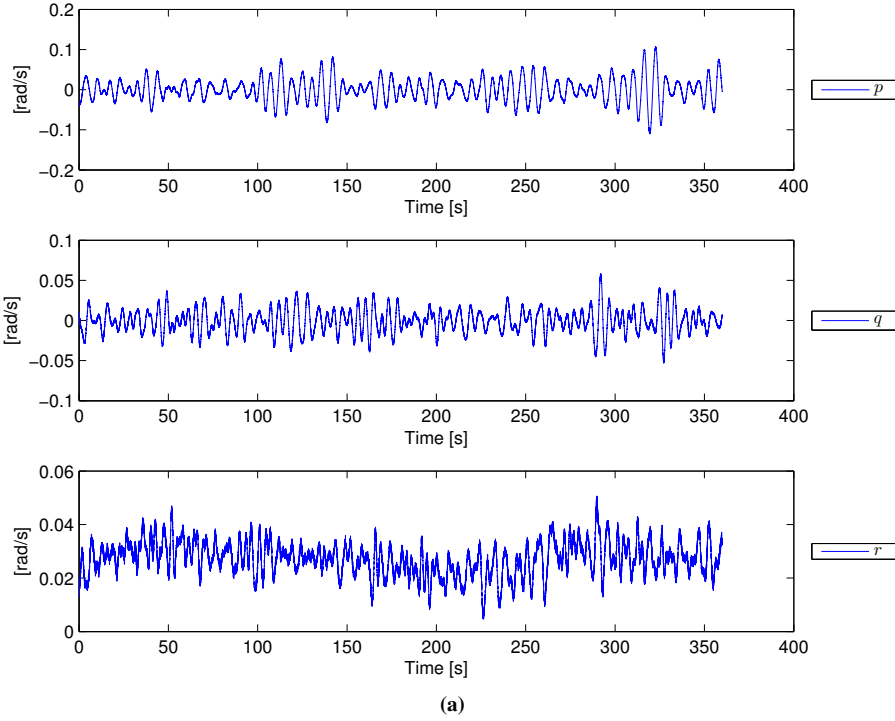


Figure 1: Plot of p , q , and r for GPS case study

Installed GPS antennas With the standard coordinate system used for ship navigation (?) (x (pos forward), y (positive stb., z (pos down), the GPS antenna from the DP system, and the GPS antennas used by the seapath have the following coordinates, measured by surveillance (?).

Table 1: GPS coordinates

Antenna	Coordinates		
	x [m](pos fwd)	y [m](pos stb)	z [m](pos down)
GPS DP	0.202	-0.611	-13.891
Seapath fwd	1.571	0.691	-13.520
Seapath aft	-0.924	0.574	-13.567

R/V Gunnerus had 3 GPS antennas installed during the sea trials, but only two measurement series are available from the data. One from the DP system, and one from MARINTEK (Seapath).

Case study 1 - Simulated GPS data

In the first case study the GPS data for two GPS antennas are simulated. The simulations are done with real data for Θ and ν , and the GPS data is generated from ??

$$P_{GPSi} = P_0 + R(t)l_i, \quad (1)$$

where (from Eq. ??)

$$\dot{P}_0 = R(t)\nu. \quad (2)$$

Lever arms with coordinates as "seapath fwd", and "seapath aft" from Table 1 are added in Eq. (1). The initial condition of the estimated arm coordinates are $[1.0m \ 0.3m \ -13.0m]^\top$, and $[-0.5m \ 0.9m \ -14.0m]^\top$. Simulation results for the Luenberger, and the adaptive observer are shown below.

Luenberger observer results The lever arm convergence results are shown below in Figure 2 and 3, and Table 2 summarize the results. The estimation of P_0 is shown in Figure 7 where a North-East plot is shown. The estimated P_0 -values are initialized at the correct value of P_0 , so the estimated and measured P_0 values are very similar during the entire simulation.

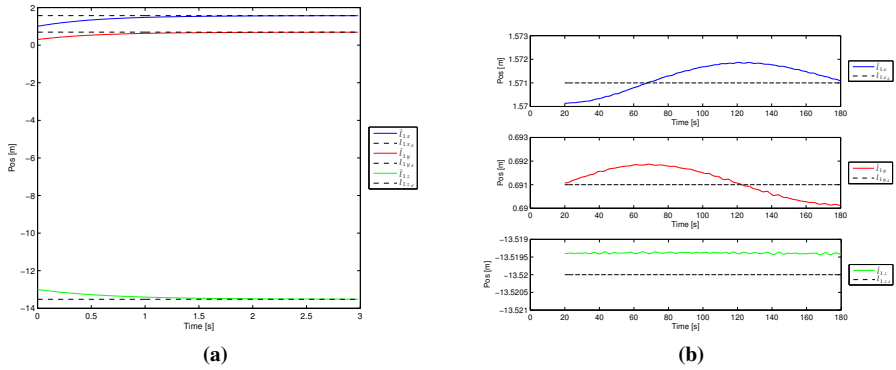


Figure 2: Lever arm coordinates, l_1 , observer, simulated GPS data

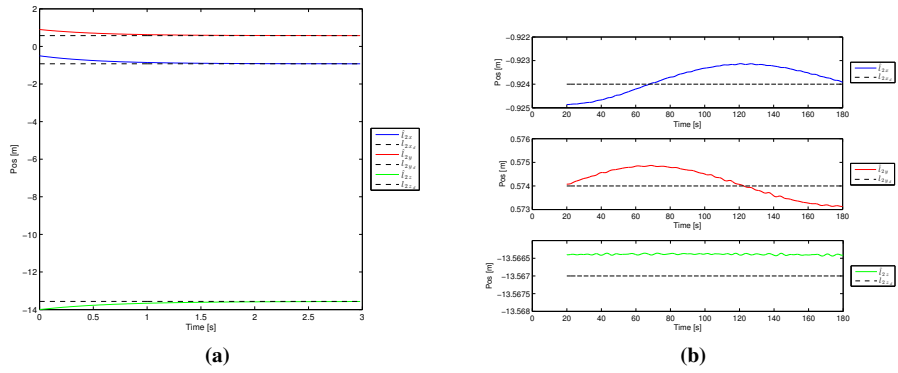


Figure 3: Lever arm coordinates, l_2 , observer, simulated GPS data

Table 2: Results, lever arm - observer, simulated GPS data

Lever arm	Lever arm coordinates						Collected from interval
	x [m]		y [m]		z [m]		
	Avg	Std. [10 ⁻⁴]	Avg	Std. [10 ⁻⁴]	Avg	Std. [10 ⁻⁵]	
1	1.5712	5.6065	0.6912	5.8248	-13.5194	1.5667	20 - 180 [s]
2	-0.9238	5.6065	0.5742	5.8248	-13.5664	1.5667	20 - 180 [s]

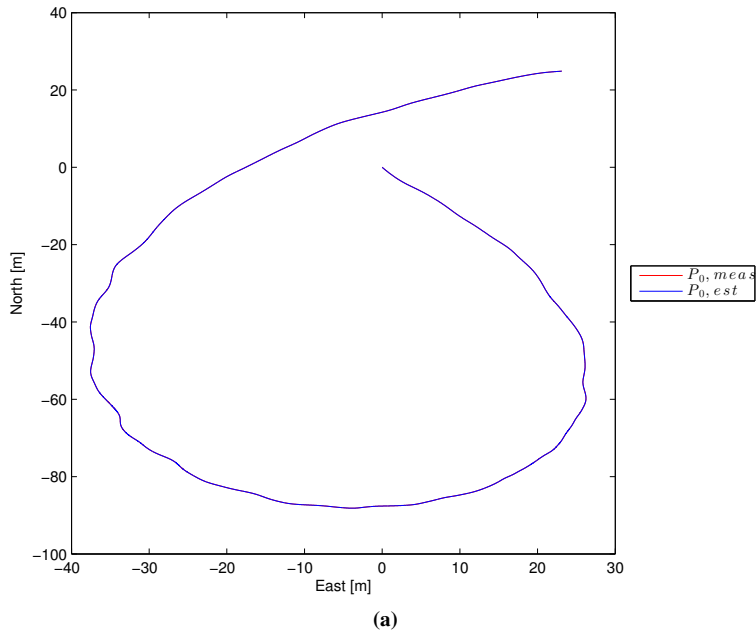


Figure 4: NE plot of P_0 , observer

Adaptive observer results The initialization of the lever arms are similar for the Luenberger, and adaptive observer, but the adaptive observer is tuned quite high such that it has a large deviation at the beginning. As seen from Figure 5 and 6, and Table 3 lever arms converge quite well, but with higher standard deviations than the Luenberger observer.

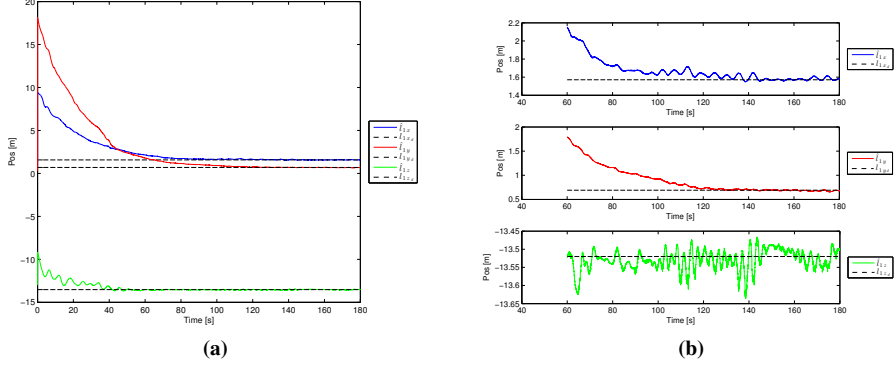


Figure 5: Lever arm coordinates, l_1 , adaptive, simulated GPS data

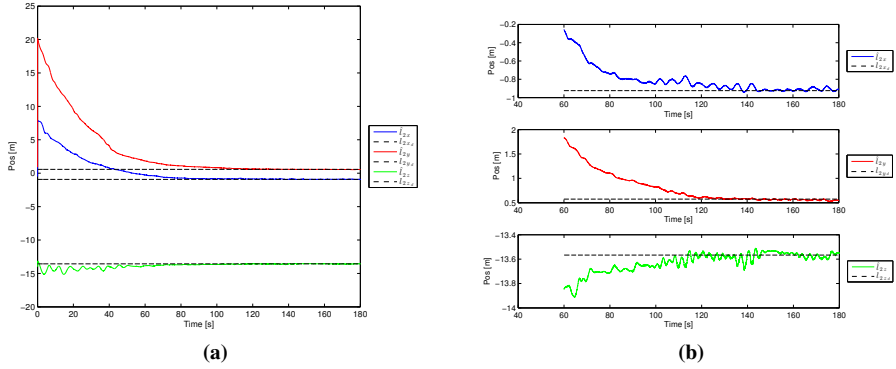


Figure 6: Lever arm coordinates, l_2 , adaptive, simulated GPS data

Table 3: Results, lever arm - adaptive, simulated GPS data

Lever arm	Lever arm coordinates						Collected from interval
	x [m]		y [m]		z [m]		
	Avg	Std.	Avg	Std.	Avg	Std.	
1	1.5787	0.0137	0.6842	0.0108	-13.5169	0.0205	150 - 180 [s]
2	-0.9132	0.0143	0.559	0.0116	-13.5636	0.0206	150 - 180 [s]

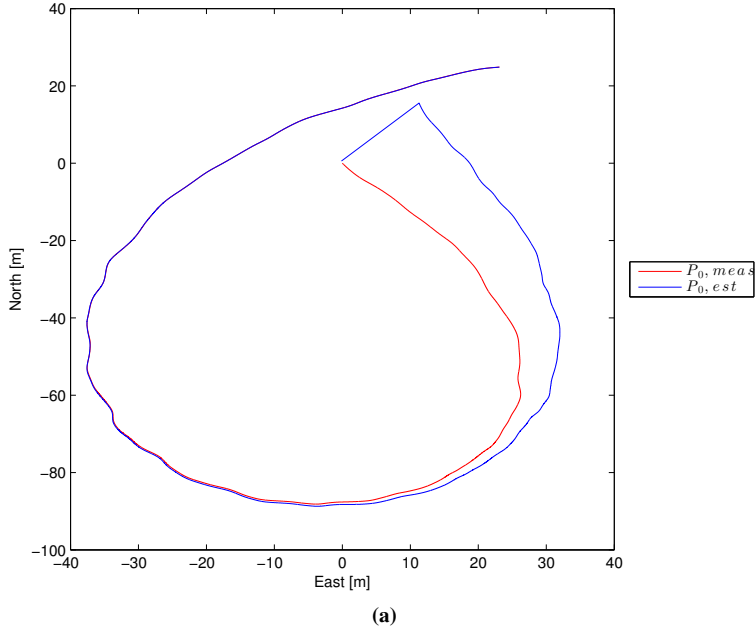


Figure 7: NE plot of P_0 , adaptive observer

Conclusive remarks The lever arms are clearly observable (and the adaptive observer is PE). Both observers have convergence in the lever arms, and the maneuver is sufficient for observability. The z -coordinate in the Luenberger observer have a (small) steady state offset, but this coordinate seems to converge for the adaptive observer, although it is a bit noisy.

Case study 2 - Real GPS data

For this case study real GPS data is used. As mentioned in the beginning of Section 0.1.1 only one GPS measurement series is available, so only one lever arm will be estimated. The GPS data is expected to be translated to a chosen point in the vessel (a chosen P_0), such that at least the lever arm coordinate in y and z -direction should converge to zero, but not necessarily in x -direction, if the chosen P_0 does not coincide with the rotation point of the vessel.

Luenberger observer results The initial conditions of the lever arm estimate are set as $[3.0m \ 2.0m \ -3.0m]^\top$. The lever arm convergence is shown in Figure 8, and values for x and z -coordinate averages are given in Table 4.

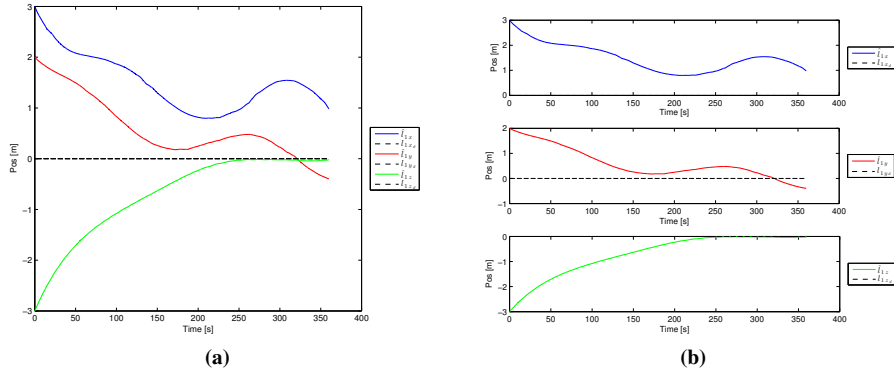


Figure 8: Lever arm coordinates, l_1 , observer, real GPS data

Table 4: Results, lever arm - observer, real GPS data

Lever arm	Lever arm coordinates						Collected from interval
	x [m]		y [m]		z [m]		
	Avg	Std.	Avg	Std.	Avg	Std.	
<i>l</i>	1.17	0.26	—	—	-0.05	0.05	130-360 [s] (x), 200-380 [s] (z)

The y -coordinate values are omitted in Table 4. The y -coordinate oscillates about zero, but it is not very clear. Higher tuning of the observer give more noise, but it is reasonable to assume that the y -value it should converge to is close to zero. Also, for the x -coordinate, it is difficult to precisely know the value it should converge to, but it appears to be close to 1.

Adaptive observer results The initial conditions of the lever arm estimate are set as $[3.0m \ 2.0m \ -1.0m]^T$.

The lever arm convergence is shown in Figure 9, and values for x and y -coordinate averages are given in Table 5.

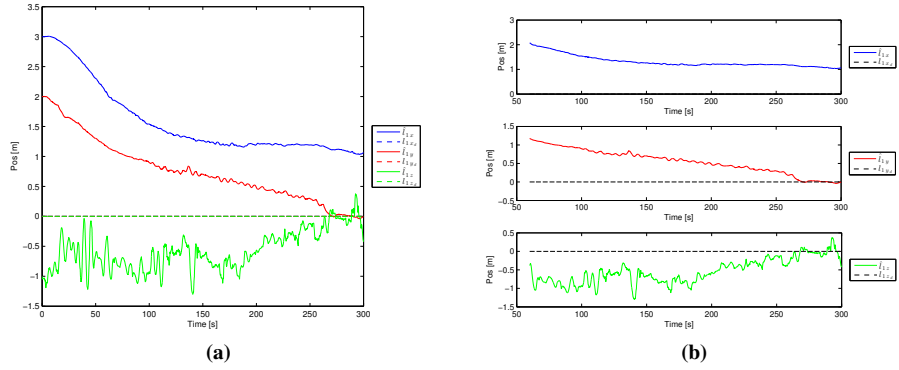


Figure 9: Lever arm coordinates, l_1 , adaptive, real GPS data

Table 5: Results, lever arm - adaptive, real GPS data

Lever arm	Lever arm coordinates						Collected from interval
	x [m]		y [m]		z [m]		
	Avg	Std.	Avg	Std.	Avg	Std.	
<i>l</i>	1.17	0.05	-0.003	0.02	—	—	170-300 [s] (x), 280-300 [s] (y)

The Γ matrix need high tuning in y and z to have convergence within the time of the maneuver performed. This makes the results noisy, and it could be interesting to perform a longer maneuver, such that lower tuning can be used. Convergence is the z -coordinate is not good.

The y -coordinate seems to converge, from Figure 9, but after 300s, the value for y goes away from zero, possibly due to low excitation in the interval after 300 seconds.

Simulated vs recorded GPS data

In

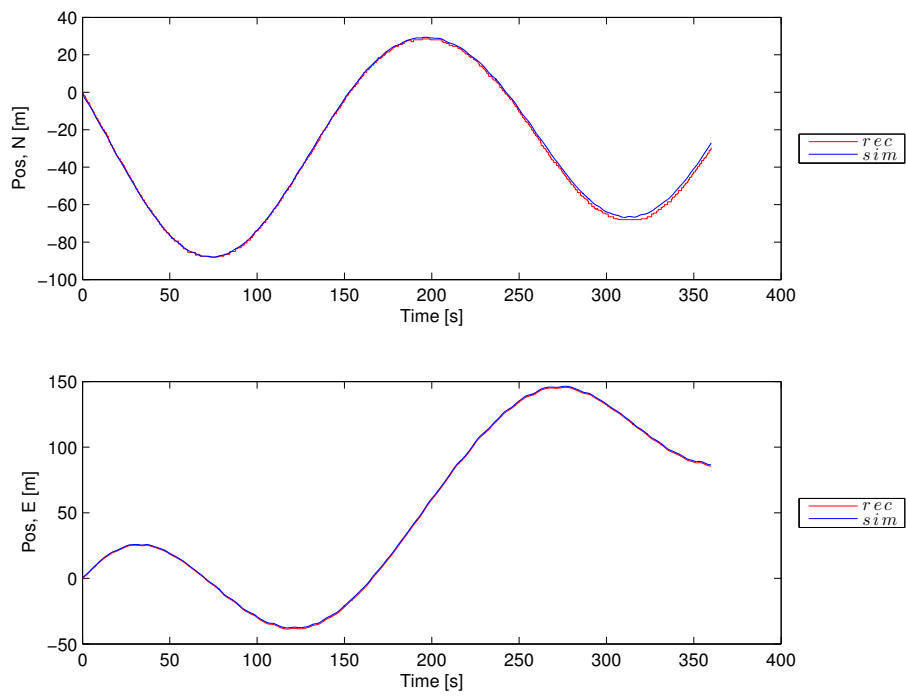


Figure 10: Comparison between real and simulated GPS data

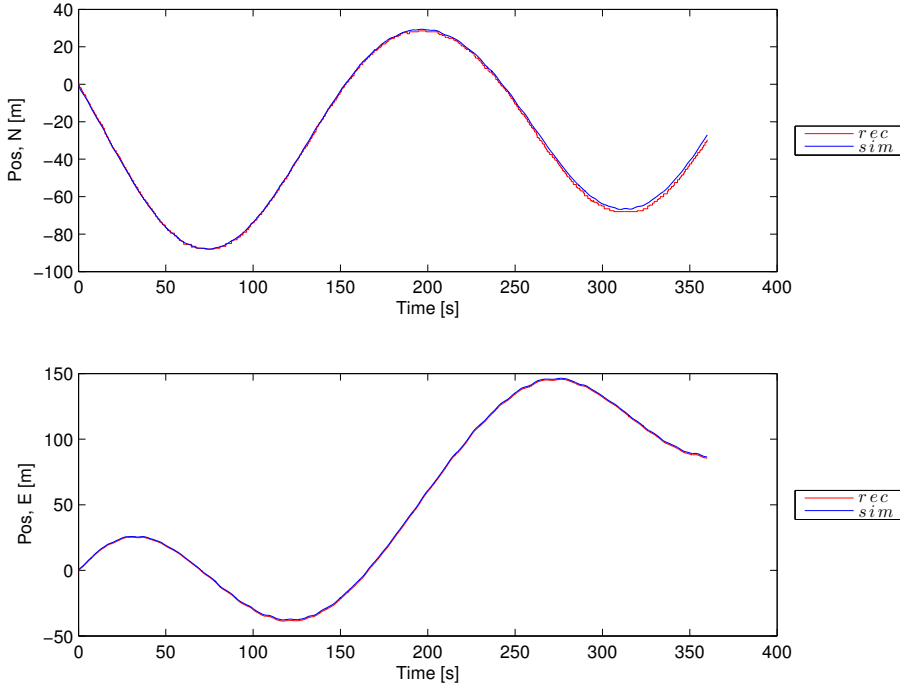


Figure 11: Comparison between real and simulated GPS data

Remarks about the lever arm convergence for real data

For both the Luenberger and the adaptive observer the lever arms converge close to the expected value. This becomes clear when the lever arm estimates are initialized far from the expected value. However, where the estimates of the lever arms were very accurate for the simulated GPS data, they are quite inaccurate for the real GPS data.

This could be explained by the difference in the simulated, and the real GPS data, as shown in Figure ???. There are small deviations between the GPS values, and this is enough for the algorithms to become less accurate.

It would be interesting with a longer maneuver, such that both observer algorithms could have time to converge with lower tuning.

0.1.2 Case study: MRU lever arms - Gunnerus data

The data used for the MRU case study is different from the one used for the GPS case studies. The reason for this is the update rate of the MARINTEK data. In August MARINTEK logs with an update rate of $100Hz$, and the MRUs also operate at $100Hz$, whereas in November MARINTEK logs with $50Hz$. The GPS has an update rate of $1Hz$, so it does

not matter whether data from November or August is used, however for the MRUs a higher update rate is desirable. The data series that is used is one of the maneuvers intended for lever arm estimation. However, this maneuver is shorter than the one used for the GPS case studies.

The values for p , q , and r are shown in Figure ?? . The yaw rate r appears to be somewhat constant, but it is higher than for the GPS case study of Section 0.1.1.

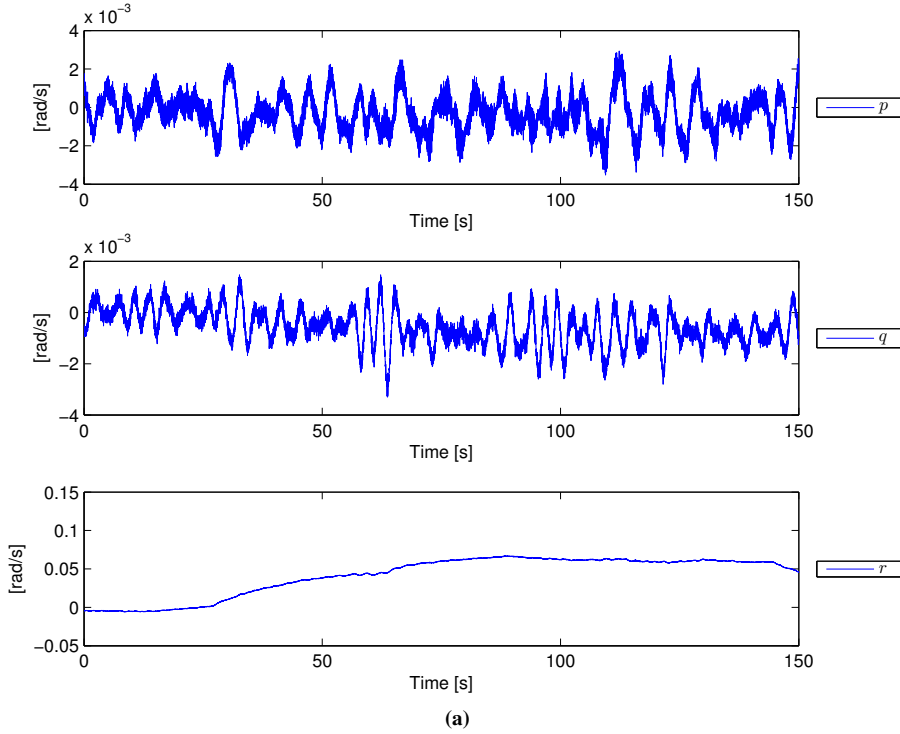


Figure 12: Plot of p , q , and r for MRU case study

Real measurements from MRU's in Gunnerus are used, and the acceleration measurements are transformed to NED-frame. There are no measurements of $\dot{\nu}$, and $\ddot{\nu}$ available. The values for $\dot{\nu}$ are found from Eq. (??) as

$$\dot{\nu} = R^\top A_0 - S\nu, \quad (3)$$

and the value of $\ddot{\nu}$ will be neglected from the observer equations in the case study.

Installed MRU's

There were 4 MRU's installed in R/V Gunnerus at the time of the sea trials, and in the case study data from two of them will be used. The lever arms of those two MRU's are given

in Table (6) below. measured by surveillance (?).

Table 6: MRU coordinates

Antenna	Coordinates		
	x [m](pos fwd)	y [m](pos stb)	z [m](pos down)
MRU 1	0.358	0.804	4.321
MRU 2	14.978	0.039	0.568

Luenberger observer results

MRU accelerations from MRU's with lever arms of coordinates

$$[0.358m \quad 0.804m \quad -4.321m]^\top,$$

and

$$[14.978m \quad 0.039m \quad 0.568m]^\top,$$

are used. The initial condition of the estimated arm coordinates are $[30m \quad 30m \quad -30.0m]^\top$, and $[30m \quad 30m \quad 30m]^\top$. The results of the observer are shown in Figure 12.

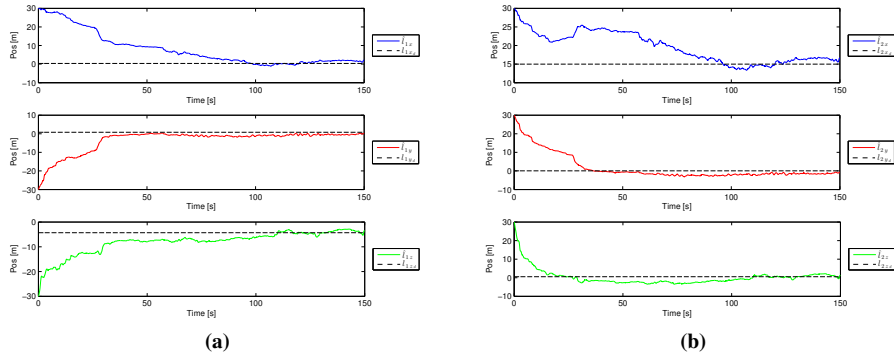


Figure 13: Lever arm coordinates l_1 (a), and l_2 (b) MRU case study

From Figure (12) is observed that the MRU estimation problem is observable. The lever arms converge quite well, and is better than for the GPS lever arms when using real data. This is probably due to the fact that the MRU's have an update rate of $100Hz$, whereas the GPS has an update rate of $1Hz$. As with the GPS problem it could be interesting with longer maneuvers to see how the observer converge with lower tuning.

Since all the lever arm results are somewhat noisy, looking at the average values does not add any value, but the result that the problem is observable is of value.